Consistent Sampling with Smoothed Quantum Walk

1st Tianyi Zhang
Department of Statistics
The University of Georgia
Athens, USA
Tianyi.Zhang@uga.edu
ORCID 0009-0007-5059-4563

2nd Yuan Ke
Department of Statistics
The University of Georgia
Athens, USA
yuan.ke@uga.edu
ORCID 0000-0001-7291-8302

***Abstract*—This paper introduces a novel sampling technique based on the dynamics of a 2-state Quantum Walk (QW) in a one-dimensional space. By leveraging concepts from nonparametric statistics, specifically the kernel smoothing method, our approach addresses two key challenges in Quantum Walk sampling: discontinuities in sampling distributions and potential inaccuracies in limiting distributions. Our innovative method effectively mitigates these issues, leading to significant improvements in density estimation and sampling efficacy compared to traditional Quantum Walk distributions and sampling techniques.**

***Index Terms*—Quantum Walk, Limit theorem, Sampling, Density estimation, Epanechnikov kernels, Transformed kernels**

I. Introduction

Quantum Walks (QWs) are analogues of classical random walks in a quantum version. They offer a wealth of concepts in this field. Like their classical counterparts, QWs can be defined as an evolution process on a graph. In classical random walks, a walker appears in definite locations (states), and their transition process stochastically depends on a probability distribution. However, in QWs, the walker is located in a superposition of states, and the evolution depends on unitary operators, which are deterministic. For a comprehensive introduction to QWs, we refer to the works of [1]–[3], and others. The limit theorems for QWs [4]–[6] also inspired the development of quantum sampling methods.

An important and fundamental mechanism in QWs is QW on a line, which is isomorphic to the evolution process on the set of all integers $\mathbb{Z}$ as defined in [7], [8]. In [9], with different initial states, the author proved limit theorems based on 2-state QW on the line, which makes it possible to sample from various target distributions, such as Semicircle distribution, Uniform distribution, Truncated Gaussian distribution, and Arcsine distribution. Despite its superior theoretical properties, at a given QW time t, 2-state QW on the line generates samples from a discrete distribution that does not have the same limiting distribution as the target distributions.

To address these challenges, kernel smoothing methods in nonparametric statistics [10]–[12] could be applied. Among various kernel functions, the Epanechnikov kernel [13] is selected in this paper, since it stands out for its optimal properties in terms of minimizing the asymptotic mean integrated square error (AMISE) with optimal bandwidth. This kernel is featured by its compact support and smoothness properties, making it a popular choice in kernel density estimation (KDE) applications. It is important to note that both the QW distributions and target distributions in our case have supports on bounded sets. Several methods have been proposed to tackle bounded set KDE problems, such as the reflection method in [14], boundary kernel method in [15], pseudo data method in [16], and Beta kernel method in [17]. In this paper, a transformation method proposed in [18] is considered. We proceed as follows: (1) We review the 2-state QW on a line and identify its limitations in sampling; (2) We review the kernel smoothing method and explain why it complements the 2-state QW on a line sampling method; (3) Using the Epanechnikov kernel and transformation method, we develop novel smoothed quantum sampling methods; (4) We demonstrate the superior empirical properties of these smoothed quantum sampling methods from extensive experiments.

Ke acknowledges the support of National Science Foundation (NSF) of the United States grants 2210468, 2243044 and 2324389.

II. Sampling with 2-state Quantum Walk on a Line

Following the state-space postulate introduced in [9], the discrete-time 2-state QW on the line resides in a tensor space $\mathcal{H}_p \otimes \mathcal{H}_c$, where $\mathcal{H}_p$ is a position Hilbert space and $\mathcal{H}_c$ is a coin Hilbert space. Further, the position space can be represented by the span of its basis states, i.e. $\mathcal{H}_p = \text{Span}\left(\{|x\rangle_p : x \in \mathbb{Z}\}\right)$, and the coin space can be represented by $\mathcal{H}_c = \text{Span}\left(\{|0\rangle_c, |1\rangle_c\}\right)$ with $\langle 0|_c = [1,0]$ and $\langle 1|_c = [0,1]$. Let $|\Psi_t\rangle$ be the superposition of 2-state QWs on the line at time $t \in \{0,1,2,\ldots\}$. We can decompose $|\Psi_t\rangle$ by

$$|\Psi_t\rangle = \sum_{x\in\mathbb{Z}} |x\rangle_p \otimes |\psi_t(x)\rangle_c \,,$$

where $|\psi_t(x)\rangle_c \in \mathcal{H}_c$. When $|\Psi_t\rangle$ is measured, the squared modulus of $|\psi_t(x)\rangle_c$ represents the probability mass function of observing the quantum walker in position x at time t.

The evolution of QWs can be viewed as a stochastic process [8] that depends on two quantum operators. First, a Hadamard operator

$$\begin{aligned} H_c &\doteq \cos\theta|0\rangle_c\langle 0| + \sin\theta|0\rangle_c\langle 1| + \sin\theta|1\rangle_c\langle 0| - \cos\theta|1\rangle_c\langle 1| \\ &= \begin{bmatrix} \cos\theta & \sin\theta \\ \sin\theta & -\cos\theta \end{bmatrix} \end{aligned} \quad (1)$$

979-8-3315-4137-8/24/$31.00 ©2024 IEEE
DOI 10.1109/QCE60285.2024.00013

with $\theta \in [0, 2\pi)$ is applied to the coin state. It is easy to check that H_c is a unitary matrix. Next, a conditional shift operator is implemented on the position state. It moves the walker one step forward if the coin state is $|1\rangle_c$ and one step backward if the coin state shows up as $|0\rangle_c$. To be specific, the conditional shift operator could be defined as

$$S_p \doteq \sum_{i\in\mathbb{Z}} |i+1\rangle_p\langle i| \otimes |1\rangle_c\langle 1| + \sum_{i\in\mathbb{Z}} |i-1\rangle_p\langle i| \otimes |0\rangle_c\langle 0|. \quad (2)$$

At time t, QWs update the current superposition $|\Psi_t\rangle$ to a new superposition $|\Psi_{t+1}\rangle$ through the following mechanism

$$|\Psi_{t+1}\rangle = S_p\left(I_p \otimes H_c\right)|\Psi_t\rangle,$$

where I_p is the identity operator on the position state.

The probability of finding the quantum walker X_t in position x at time t can be calculated by

$$\mathbb{P}\left(X_t = x\right) = \langle\psi_t(x)|\psi_t(x)\rangle_c. \quad (3)$$

Utilizing the discrete-time Fourier transformation, we define

$$|\hat{\Psi}_t(k)\rangle_c = \sum_{x\in\mathbb{Z}} e^{-ikx}|\psi_t(x)\rangle_c, \quad \text{for } k \in [-\pi, \pi).$$

Subsequently, we can define the inverse transformation as

$$|\psi_t(x)\rangle_c = \frac{1}{2\pi}\int_{-\pi}^{\pi} |\hat{\Psi}_t(k)\rangle_c e^{ikx} dk.$$

Similar to the discussions in [9], the mathematical formulations above motivate a quantum sampling scheme to generate a random sample of the target distribution by matching the moments of the distribution.

Let $F : \mathbb{R} \mapsto \mathbb{R}$ be a real function satisfying

1) $F(k + 2\pi) = F(k)$,
2) $\int_{-\pi}^{\pi} F(k)^2 dk = 2\pi$,
3) $F(k) \in C^\infty[-\pi, \pi]$ almost everywhere,
4) $|F(k - \pi)| = |F(-k)| = |F(k)|$.

We introduce a non-localized initial state

$$|\hat{\Psi}_0(k)\rangle_c = F(k)(\alpha|0\rangle_c + \beta|1\rangle_c),$$

or equivalently

$$|\psi_0(x)\rangle_c = \left[\frac{1}{2\pi}\int_{-\pi}^{\pi} F(k)e^{ikx}dk\right](\alpha|0\rangle_c + \beta|1\rangle_c)$$

with $\alpha, \beta \in \mathbb{C}$ and $|\alpha|^2 + |\beta|^2 = 1$.

Let r be a non-negative integer, $c = \cos\theta$, $s = \sin\theta$, and $\Re(z)$ be the real part of $z \in \mathbb{C}$. The limiting moments of X_t/t satisfy

$$\lim_{t\to\infty}\mathbb{E}\left[\left(\frac{X_t}{t}\right)^r\right] = \int_{\mathbb{R}} x^r f(x;\alpha,\beta)F(\kappa(x))^2\mathbb{I}_{(-|c|,|c|)}(x)dx,$$

where

$$f(x;\alpha,\beta) = \frac{|s|}{\pi\left(1-x^2\right)\sqrt{c^2-x^2}} \cdot \left[1 - \left\{|\alpha|^2 - |\beta|^2 + \frac{2s\Re(\alpha\bar{\beta})}{c}\right\}x\right],$$

$$\kappa(x) = \arccos\left(\frac{|s|x}{c\sqrt{1-x^2}}\right),$$

$$\text{and } \mathbb{I}_{(-|c|,|c|)}(x) = \begin{cases} 1 & \text{if } x \in (-|c|,|c|) \\ 0 & \text{otherwise} \end{cases}.$$

Moreover, if α, β are properly selected such that $|\alpha|^2 - |\beta|^2 + \frac{2s\Re(\alpha\bar{\beta})}{c} = 0$ (e.g. $\alpha = \frac{\sqrt{2}}{2}, \beta = \frac{\sqrt{2}}{2}i$), one can choose the form of F to control the (scaled) limiting moments of X_t. Given a properly chosen initial state $|\psi_0(x)\rangle_c$, we can generate $\frac{X_{t,i}}{t}$, $i = 1, \cdots, N$, as a random sample from a target distribution. Here we list a few examples.

1) **Wigner semicircle law**:
Choose $F(k) = \frac{\sqrt{2|s|^3}\sin k}{1-c^2\sin^2 k}$. Then,
$$\lim_{t\to\infty}\mathbb{E}\left[\left(\frac{X_t}{t}\right)^r\right] = \int_{(-|c|,|c|)} x^r \frac{2\sqrt{c^2-x^2}}{\pi c^2}dx;$$

2) **Uniform distribution**:
Choose $F(k) = \sqrt{\frac{\pi s^2|\sin k|}{2(1-c^2\sin^2 k)^{\frac{3}{2}}}}$. Then,
$$\lim_{t\to\infty}\mathbb{E}\left[\left(\frac{X_t}{t}\right)^r\right] = \int_{(-|c|,|c|)} x^r \frac{1}{2|c|}dx;$$

3) **Truncated Gaussian distribution**:
Choose
$F(k) = \sqrt{\frac{\sqrt{2\pi}|c|s^2|\sin k|}{2\sigma\,\mathrm{erf}\left(\frac{|c|}{\sqrt{2}\sigma}\right)(1-c^2\sin^2 k)^{\frac{3}{2}}}}\exp\left\{-\frac{c^2\cos^2 k}{4\sigma^2(1-c^2\sin^2 k)}\right\}$.
Then,
$$\lim_{t\to\infty}\mathbb{E}\left[\left(\frac{X_t}{t}\right)^r\right] = \int_{(-|c|,|c|)} x^r \frac{\exp\left(-\frac{x^2}{2\sigma^2}\right)}{\sqrt{2\pi}\sigma\,\mathrm{erf}\left(\frac{|c|}{\sqrt{2}\sigma}\right)}dx,$$
where $\mathrm{erf}(\cdot)$ is the Gaussian error function, and $\sigma > 0$ stands for the standard deviation;

4) **Arcsine law**:
Choose $F(k) = \sqrt{\frac{|s|}{1-c^2\sin^2 k}}$. Then,
$$\lim_{t\to\infty}\mathbb{E}\left[\left(\frac{X_t}{t}\right)^r\right] = \int_{(-|c|,|c|)} x^r \frac{1}{\pi\sqrt{c^2-x^2}}dx.$$

For most cases, the preparation of the initial state $|\psi_0(x)\rangle_c$ would not be complex. For example, considering Wigner semicircle law, Uniform distribution, or Truncated Gaussian distribution, even if the non-localized initial state cannot be generated accurately, preparing the initial state $|\psi_0(x)\rangle_c$ only for those x close to 0 would be enough, and it would approximate the true initial state on $\mathbb{Z}$ with arbitrarily tiny difference. However, this quantum sampling scheme has two limitations as shown in Fig. 1. On the one hand, at a finite time t, $\frac{X_t}{t}$ actually approximates a continuous target distribution on

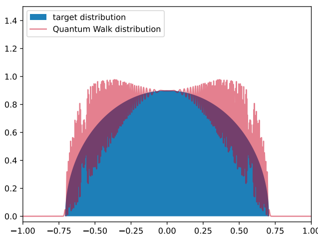

(a) Semicircle law, $t = 1000$.

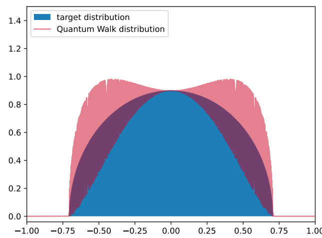

(b) Semicircle law, $t = 5000$.

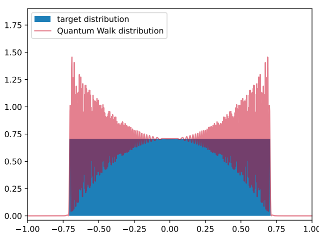

(c) Uniform distribution, $t = 1000$.

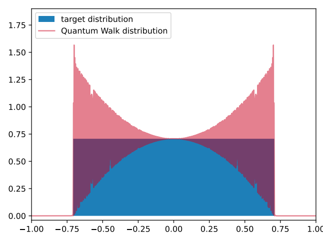

(d) Uniform distribution, $t = 5000$.

Fig. 1: Quantum Walk distributions and target distributions. Four patterns are plotted for different approximation laws and t values. The red lines are the true probability distributions of the Quantum Walk sample $\frac{X_t}{t}$. The blue areas are PDFs of the target distributions.

the set $(-|c|, |c|)$ by an empirical discrete distribution on the set $\left\{\frac{i}{t} : i \in \mathbb{Z} \cap (-|c| \cdot t, |c| \cdot t)\right\}$. This approximation error may create bias and hence yield sub-optimal finite-sample performance. On the other hand, the analysis above only provides the asymptotic behavior of the (scaled) moments. The limiting distribution of X_t (or of $\frac{X_t}{t}$), as a more desired theoretical result, is still lacking. Denote $f_{\text{target}}(\cdot)$ as the probability density function (PDF) of the target distribution. It is not guaranteed that $\forall x \in (-|c|, |c|)$, $\lim_{t\to\infty} \mathbb{P}\left(\frac{X_t}{t} = x\right) = f_{\text{target}}(x)$. In fact, in many cases, $\lim_{t\to\infty} \mathbb{P}\left(\frac{X_t}{t} = x\right)$ does not even exist. To overcome these two limitations, we propose to inovate the quantum sampling method by borrowing the wisdom from the statistical kernel smoothing techniques.

III. Kernel Smoothing

In the realm of nonparametric statistics, kernel smoothing is a widely used technique to obtain estimates through a weighted average of a "localized" neighborhood in the random sample, see [10], [19]–[21] and reference therein. A Kernel function $K(\cdot)$ is usually introduced to assign weights and u usually represents the "closeness" between two observations. The size of the local neighborhood is controlled by a bandwidth (or smoothing) parameter h that can converge to 0 when the sample size n diverges. For example, a popular choice of the kernel function in nonparametric regression is the Epanechnikov kernel which achieves a high minimax efficiency [22]. To be specific, the Epanechnikov kernel is defined as

$$K(u) = \frac{3}{4}\left(1 - u^2\right)_+, \tag{4}$$

where $(a)_+ = a$ if $a \geq 0$ and $(a)_+ = 0$ if $a < 0$.

Let $X_1 \ \ldots,\ X_n$ be an independent and identically distributed (i.i.d.) sample drawn from a probability density function $f(\cdot)$. A kernel smoothing density estimator of $f(\cdot)$ is defined as follows.

$$\hat{f}(x) = \frac{1}{n}\sum_{i=1}^{n} K_h\left(x, X_i\right), \tag{5}$$

where $K_h(x, y) = h^{-1}K\{(x-y)/h\}$.

Under mild conditions, the kernel density estimator enjoys the following two nice statistical properties:

1) $\lim_{n\to\infty} \mathbb{E}\left[\hat{f}(x)\right] = f(x)$,
2) $\lim_{n\to\infty} \mathrm{Var}\left[\hat{f}(x)\right] = 0$.

Further, one can prove that kernel density estimator converges in probability to true density funciton, i.e. $\forall x$, $\hat{f}(x) \xrightarrow{p} f(x)$. Therefore, we plan to borrow the wisdom of kernel smoothing to overcome the limitations of the quantum sampling method as discussed in Section II.

IV. Kernel Smoothed Quantum Sampling

In this section, we introduce a novel quantum sampling method by integrating quantum walk and kernel smoothing. Throughout this section, we denote $f^*(\cdot)$ the density function of the target distribution, $X_{t,i}$ the location of ith quantum walker at time t, and $Y_{t,i} = \frac{X_{t,i}}{t}$ for $i = 1, \ \ldots,\ N$ and $t \in \mathbb{Z}^+$.

With the Epanechnikov kernel, we can define a kernel smoothing density estimator of the target distribution $f^*(\cdot)$ as

$$\hat{f}_0(x) = \frac{1}{Nh}\frac{3}{4}\sum_{i=1}^{N}\left(1 - \left(\frac{x - Y_{t,i}}{h}\right)^2\right)_+.$$

As discussed in Section II, the support of the target distribution for quantum sampling is usually a bounded interval $(-|c|, |c|)$. However, the support of $\hat{f}_0(\cdot)$ is the whole real line. To make the two supports match, we rescale $\hat{f}_0(\cdot)$ by

$$\hat{f}_1(x) = \frac{\hat{f}_0(x)}{\int_{(-|c|,|c|)} \hat{f}_0(z)dz}. \tag{6}$$

We call $\hat{f}_1(x)$ the Smoothed Quantum Sampling (SQS). According to the empirical experiments to be unveiled in Section V, SQS suffers from biases in the boundary areas.

To reduce the bias in the boundary area, we propose a Transformed Smoothed Quantum Sampling (TSQS). Let $T_c : (-|c|, |c|) \mapsto \mathbb{R}$ be a monotonically increasing function which is three times continuously differentiable. Such a $T_c(\cdot)$ function is easy to find or construct. For example, one can choose $T_c(\cdot)$ as the inverse of a Gaussian distribution function

$$T_{c,1}(x) = \Phi^{-1}\left(\frac{x + |c|}{2|c|}\right), \tag{7}$$

where $\Phi(\cdot)$ is the cumulative distribution function of standard Gaussian. As another example, one can choose $T_c(\cdot)$ to be a logit function such as

$$T_{c,2}(x) = \mathrm{logit}\left(\frac{x + |c|}{2|c|}\right) = \ln\frac{x + |c|}{|c| - x}.$$

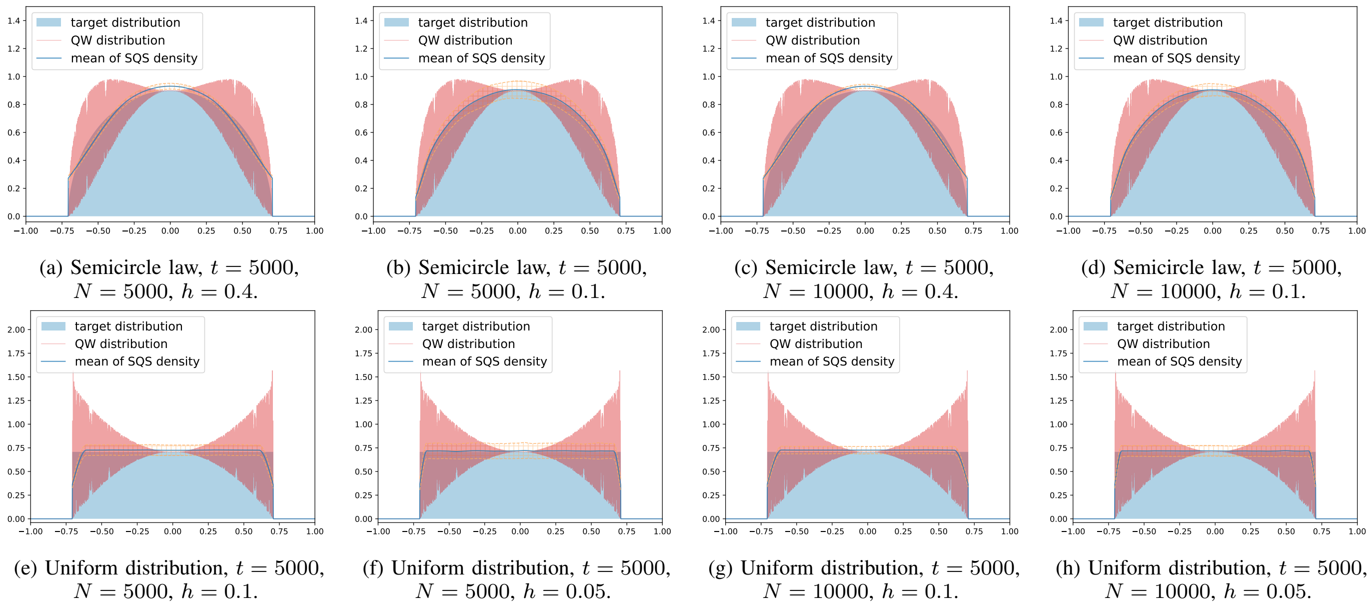

(a) Semicircle law, $t = 5000$, $N = 5000$, $h = 0.4$.
(b) Semicircle law, $t = 5000$, $N = 5000$, $h = 0.1$.
(c) Semicircle law, $t = 5000$, $N = 10000$, $h = 0.4$.
(d) Semicircle law, $t = 5000$, $N = 10000$, $h = 0.1$.
(e) Uniform distribution, $t = 5000$, $N = 5000$, $h = 0.1$.
(f) Uniform distribution, $t = 5000$, $N = 5000$, $h = 0.05$.
(g) Uniform distribution, $t = 5000$, $N = 10000$, $h = 0.1$.
(h) Uniform distribution, $t = 5000$, $N = 10000$, $h = 0.05$.

Fig. 2: SQS densities. Graph matrix with eight patterns are plotted for different approximation law, sample size N, and bandwidth h. The light blue lines are the mean functions of Epanechnikov kernel estimators with 500 replications. The orange cross-shaded areas represent the area given by $\text{mean} \pm 2 \times \text{standard error}$. The red lines are the true probability distributions of the Quantum Walk sample $Y_{t,i}$. The blue areas are PDFs of the target distributions.

With a properly chosen transformation function $T_c(\cdot)$, we define the TSQS estimator by

$$\hat{f}_2(x) = T_c'(x) \cdot \frac{1}{Nh} \frac{3}{4} \sum_{i=1}^{N} \left(1 - \left(\frac{T_c(x) - T_{t,i}}{h} \right)^2 \right)_+ , \quad (8)$$

where $T_{t,i} = T_c(Y_{t,i})$, and $T_c'(\cdot)$ represents the first order derivative of $T_c(\cdot)$.

V. Experiments

In this section, we use several numerical experiments to validate the concepts discussed in the paper. We will also assess and compare the empirical performances of Quantum Walk (QW), Smoothed Quantum Sampling (SQS), and Transformed Smoothed Quantum Sampling (TSQS) in various scenarios. Throughout this section, we set $\alpha = \frac{\sqrt{2}}{2}, \beta = \frac{\sqrt{2}}{2} i$, and $\theta = \frac{\pi}{4}$.

A. Empirical analysis for Quantum Sampling Performance

In the first experiment, we assess the empirical performances of SQS and TSQS under various settings. We will also compare SQS and TSQS with QW and the target distribution. We choose the Wigner semicircle law and the Uniform distribution as introduced in Section II as the target distributions. We set the running time of QW to be $t = 5,000$ and the sample size to be $N = 5,000$ and $10,000$. For SQS and TSQS, we use the Epanechnikov kernel and evaluate their performances with both large and small smoothing parameters. Specifically, we choose $h = 0.4$ and 0.1 for the Wigner semicircle law and choose $h = 0.1$ and 0.05 for the Uniform distribution. For TSQS, we choose the inverse Gaussian transformation function $T_{c,1}(\cdot)$ defined as in (7). For each scenario, we repeat 500 replications. The experiment results for SQS and TSQS are reported in Fig. 2 and Fig. 3, respectively.

The experiment results clearly show that with a given time t, the samples generated by both SQS and TSQS, with well-chosen N and smoothing parameter h, are much closer to the target density compared to the samples generated from QW, thanks to the bias correction made by kernel smoothing. Correspondingly, the samples generated by SQS and TSQS converge to the target density as t and N increase. Still, the choice of the smoothing parameter plays an important role in smoothed quantum sampling methods to control the bias-variance trade-off. A large value of h creates a smoother estimate which may have low variance but a bias. Conversely, a small value of h produces a more "localized" estimate which may have a small bias but can suffer from larger variance. In practice, we can choose h through a multi-fold cross-validate approach.

Furthermore, as shown in Fig. 2, both QW and SQS suffer from the boundary bias issue. For the Wigner semicircle law experiment, $\hat{f}_1(\cdot)$ shows densities outside $(-|c|, |c|)$, indicating that $\hat{f}_1(x) > 0$ when $x = -|c|$ or $x = |c|$, by the continuity of $\hat{f}_1(x)$. This results in a positive bias at the boundary for the samples generated by SQS. For the Uniform distribution case, when x is close to the boundaries, $\hat{f}_1(x)$ only uses interior observations, leading to an underestimation of the target density and hence a negative bias. Although this issue diminishes as $N \to \infty$ and $h \to 0$, it remains significant in practice with a finite sample. We are happy to see, from Fig. 3, this boundary bias issue is mitigated by TSQS as we expected.

B. Statistical analysis for Quantum Sampling Performance

Next, we make a statistical inference analysis for quantum sampling methods. We use the Kolmogorov–Smirnov (KS) test to determine if the observations (of size m) generated from a quantum sampling method originates from the target

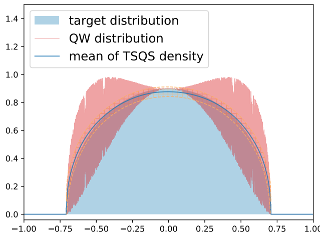

(a) Semicircle law, $t = 5000$, $N = 5000$, $h = 0.4$.

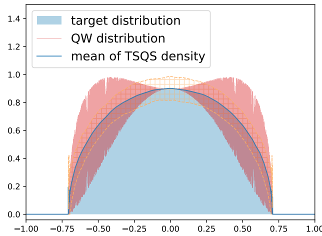

(b) Semicircle law, $t = 5000$, $N = 5000$, $h = 0.1$.

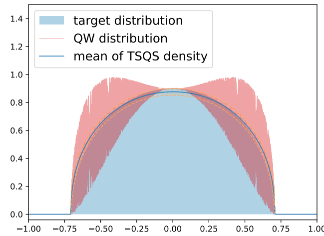

(c) Semicircle law, $t = 5000$, $N = 10000$, $h = 0.4$.

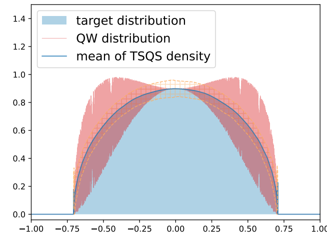

(d) Semicircle law, $t = 5000$, $N = 10000$, $h = 0.1$.

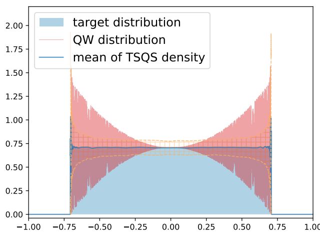

(e) Uniform distribution, $t = 5000$, $N = 5000$, $h = 0.1$.

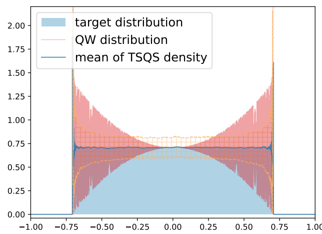

(f) Uniform distribution, $t = 5000$, $N = 5000$, $h = 0.05$.

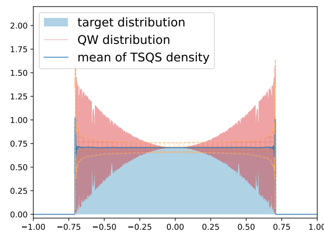

(g) Uniform distribution, $t = 5000$, $N = 10000$, $h = 0.1$.

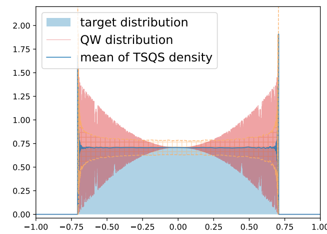

(h) Uniform distribution, $t = 5000$, $N = 10000$, $h = 0.05$.

Fig. 3: TSQS densities. Graph matrix with eight patterns are plotted for different approximation law, sample size N, and bandwidth h. The light blue lines are the mean functions of Epanechnikov kernel estimators with 500 replications. The orange cross-shaded areas represent the area given by $\text{mean} \pm 2 \times \text{standard error}$. The red lines are the true probability distributions of the Quantum Walk sample $Y_{t,i}$. The blue areas are PDFs of the target distributions.

distribution. The KS test is a nonparametric test for the equivalence of two continuous one-dimensional probability distributions. In the context of our study, the KS test evaluates how well the sample distributions conform to theoretical distributions by comparing their cumulative distribution functions. The p-values from the KS test indicate the probability that the observed differences between the sample and reference distributions could occur by chance. A high p-value suggests a lack of evidence against the null hypothesis that the sample distribution matches the target distribution.

We consider a similar experiment setting as Section V-A. We set $t = 5000$ and $N = 200000$ for QW. We also set the sample size of the obsevations in KS tests to be $m = 50,000$, $200,000$ and $500,000$. For the Wigner semicircle law case, we choose $h = 0.02$ for SQS and $h = 0.05$ for TSQS. For the Uniform distribution case, we choose $h = 0.006$ for SQS and $h = 0.08$ for TSQS. The histograms of p-values over 500 replications are presented in Fig. 4. When the null hypothesis of the KS test is true, the p-value of the test statistic should follow a uniform distribution between 0 and 1. In Fig. 4, the QW samples and SQS samples exhibit comparable performance when N is small, with all methods displaying evenly distributed p-values across $[0, 1]$. However, as N increases, all methods tend to fail as their p-values concentrate increasingly towards 0. Notably, TSQS samples are preferable since their p-values are less biased towards 0 compared to the QW and SQS samples. This suggests that TSQS samples better approximate the target distributions as sample sizes increase.

VI. Discussion and Future Work

Although the experiments in Section V show SQS and TSQS exhibit superior empirical performances in statistical sampling, the theoretical properties of these methods are yet to be investigated, which is our main research focus in the next stage. Here we propose a few research objectives we aim to investigate in future work. As discussed in Subsection III, we would like to show that SQS and TSQS satisfy the convergence in probability. For $i = 1, 2$ and $\forall x$, we aim to prove

1) $\lim_{(N,t)\to\infty} \mathbb{E}\left[\hat{f}_i(x)\right] = f_{\text{target}}(x)$,
2) $\lim_{(N,t)\to\infty} \mathrm{Var}\left[\hat{f}_i(x)\right] = 0$.

Additionally, as discussed in Subsection V-A, selecting the smoothing parameter h is crucial for the practical application of the method. This process typically involves determining the expected L_2 risk function, also known as the mean integrated squared error (MISE),

$$\mathrm{MISE}_{t,N,i}(h) = \mathbb{E}\left\{\int_{-|c|}^{|c|}\left[\hat{f}_i(x) - f_{\text{target}}(x)\right]^2 dx\right\},$$

for given t, N, and $i = 1, 2$. The explicit form of MISE is often difficult to derive, and as an alternative, its asymptotic version, AMISE, is used:

$$\begin{aligned}&\mathrm{AMISE}_{t,N,i}(h)\\ &= \int_{-|c|}^{|c|} \mathrm{Bias}^2\left[\hat{f}_i(x)\right] + \mathrm{Var}\left[\hat{f}_i(x)\right] dx\\ &= \int_{-|c|}^{|c|} \left\{\mathbb{E}\left[\hat{f}_i(x)\right] - f_{\text{target}}(x)\right\}^2 + \mathrm{Var}\left[\hat{f}_i(x)\right] dx.\end{aligned}$$

Consequently, the smoothing parameter h can be selected by finding $h^* = \arg\min_h \mathrm{AMISE}_{t,N,i}(h)$.

References

[1] J. Kempe, “Quantum random walks: an introductory overview,” *Contemporary Physics*, vol. 44, no. 4, pp. 307–327, 2003.

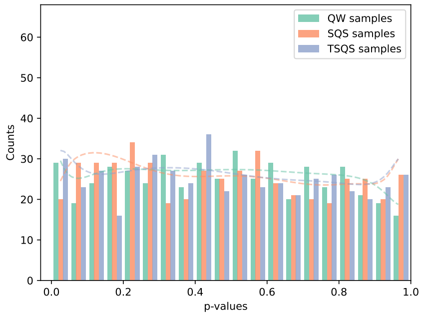

(a) Semicircle law, $m = 50000$.

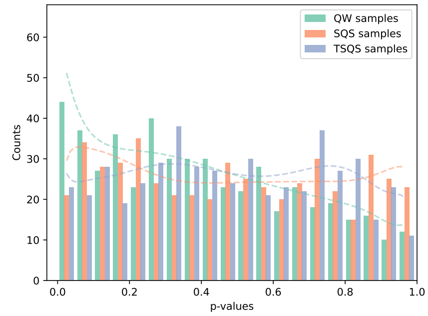

(b) Semicircle law, $m = 200000$.

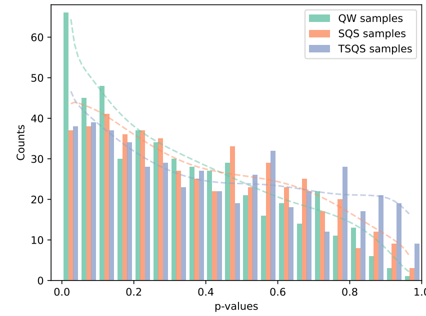

(c) Semicircle law, $m = 500000$.

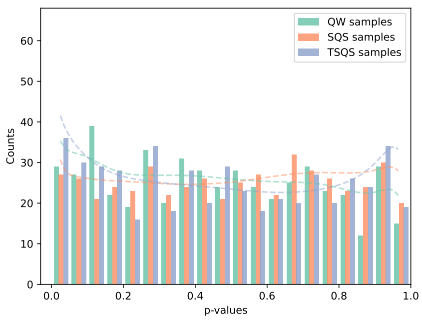

(d) Uniform distribution, $m = 50000$.

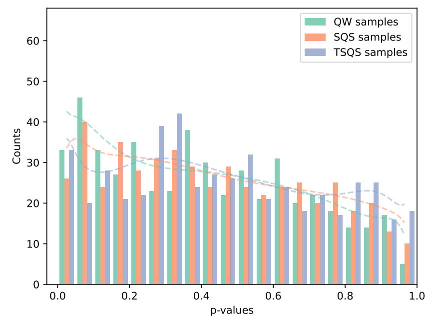

(e) Uniform distribution, $m = 200000$.

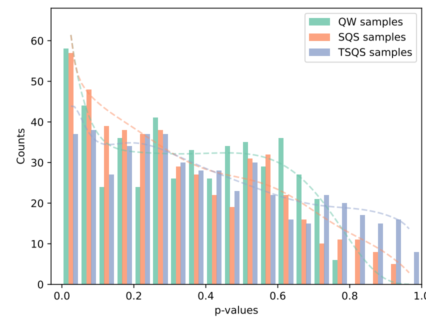

(f) Uniform distribution, $m = 500000$.

Fig. 4: Histograms and distributions of p-values of KS tests on QW samples and SQS samples. Six patterns are plotted for different approximation laws and different sample sizes m of observations in KS tests. Green bars and lines are from QW samples. Orange bars and lines are from SQS samples. Blue bars and lines are from TSQS samples.

[2] D. Aharonov, A. Ambainis, J. Kempe, and U. Vazirani, "Quantum walks on graphs," in *Proceedings of the thirty-third annual ACM symposium on Theory of computing*, 2001, pp. 50–59.

[3] S. Venegas-Andraca, *Quantum walks for computer scientists*. Springer Nature, 2022.

[4] K. Chisaki, M. Hamada, N. Konno, and E. Segawa, "Limit theorems for discrete-time quantum walks on trees," *Interdisciplinary Information Sciences*, vol. 15, no. 3, pp. 423–429, 2009.

[5] S. Attal, N. Guillotin-Plantard, and C. Sabot, "Central limit theorems for open quantum random walks and quantum measurement records," in *Annales Henri Poincaré*, vol. 16. Springer, 2015, pp. 15–43.

[6] N. Konno, "Limit theorem for continuous-time quantum walk on the line," *Physical Review E*, vol. 72, no. 2, p. 026113, 2005.

[7] A. Nayak and A. Vishwanath, "Quantum walk on the line," 2000.

[8] S. E. Venegas-Andraca, "Quantum walks: a comprehensive review," *Quantum Information Processing*, vol. 11, no. 5, pp. 1015–1106, 2012.

[9] T. Machida, "Realization of the probability laws in the quantum central limit theorems by a quantum walk," *Quantum Info. Comput.*, vol. 13, no. 5–6, p. 430–438, may 2013.

[10] M. P. Wand and M. C. Jones, *Kernel smoothing*. CRC press, 1994.

[11] D. W. Scott, *Multivariate density estimation: theory, practice, and visualization*. John Wiley & Sons, 2015.

[12] B. W. Silverman, *Density estimation for statistics and data analysis*. Routledge, 2018.

[13] V. A. Epanechnikov, "Non-parametric estimation of a multivariate probability density," *Theory of Probability & Its Applications*, vol. 14, no. 1, pp. 153–158, 1969.

[14] E. F. Schuster, "Incorporating support constraints into nonparametric estimators of densities," *Communications in Statistics-Theory and methods*, vol. 14, no. 5, pp. 1123–1136, 1985.

[15] T. Gasser and H.-G. Müller, "Kernel estimation of regression functions," in *Smoothing Techniques for Curve Estimation: Proceedings of a Workshop held in Heidelberg, April 2–4, 1979*. Springer, 1979, pp. 23–68.

[16] A. Cowling and P. Hall, "On pseudodata methods for removing boundary effects in kernel density estimation," *Journal of the Royal Statistical Society Series B: Statistical Methodology*, vol. 58, no. 3, pp. 551–563, 1996.

[17] S. X. Chen, "Beta kernel estimators for density functions," *Computational Statistics & Data Analysis*, vol. 31, no. 2, pp. 131–145, 1999.

[18] J. S. Marron and D. Ruppert, "Transformations to reduce boundary bias in kernel density estimation," *Journal of the Royal Statistical Society: Series B (Methodological)*, vol. 56, no. 4, pp. 653–671, 1994.

[19] E. A. Nadaraya, "On estimating regression," *Theory of Probability & Its Applications*, vol. 9, no. 1, pp. 141–142, 1964.

[20] G. S. Watson, "Smooth regression analysis," *Sankhyā: The Indian Journal of Statistics, Series A (1961-2002)*, vol. 26, no. 4, pp. 359–372, 1964. [Online]. Available: http://www.jstor.org/stable/25049340

[21] J. Fan, *Local polynomial modelling and its applications: monographs on statistics and applied probability 66*. Routledge, 1996.

[22] ——, "Design-adaptive nonparametric regression," *Journal of the American Statistical Association*, vol. 87, no. 420, pp. 998–1004, 1992. [Online]. Available: http://www.jstor.org/stable/2290637